A&A 462, L37–L40 (2007)
DOI: 10.1051/0004-6361:20066611

Astronomy & Astrophysics

Letter to the Editor

Probing the close environment of massive young stars with spectro-astrometry

J. M. C. Grave[1,2] and M. S. N. Kumar[1]

[1] Centro de Astrofísica da Universidade do Porto, Rua das Estrelas, 4150-762 Porto, Portugal
[2] Departamento de Matemática Aplicada da Faculdade de Ciências da Universidade do Porto, Portugal
e-mail: [jgrave;nanda]@astro.up.pt

Received 20 October 2006 / Accepted 6 December 2006

ABSTRACT

Aims. We test the technique of spectro-astrometry to investigate the close environment of massive young stellar objects (MYSOs).
Methods. Archival VLT near infrared K band spectra ($R = 8900$) of three massive young stellar objects and one Wolf-Rayet star are examined for spectro-astrometric signatures. The young stellar objects display emission lines such as Brγ, CO 2–0 and CO 3–1 that are characteristic of ionised regions and molecular disks respectively. Two of the sample sources also display emission lines such as NIII and MgII that are characteristic of high temperatures.
Results. Most of the emission lines show spectro-astrometric signal at various levels resulting in different positional displacements. The shapes and magnitudes of the positional displacements imply the presence of large disks/envelopes in emission and expanding shells of ionised gas. The results obtained for the source 18006-2422nr766 in particular provide larger estimates (>300 AU) for CO emitting regions, indicating that in MYSOs, CO may also arise from inner regions of extended dense envelopes.
Conclusions. The overall results from this study demonstrate the utility of spectro-astrometry to constrain the sizes of physical entities such as disks/envelopes, UCHII regions and/or ionised shells in the close environment of a massive young star.

Key words. techniques: spectroscopic – stars: formation – ISM: HII regions – line: profiles – methods: observational

1. Introduction

The technique of spectro-astrometry (SA) has been explored in the past few years due to its potential to address important astrophysical problems. It has been successfully applied to the detection of pre-main sequence binaries (Bailey 1998b; Takami et al. 2003; Baines et al. 2006), the study of young stellar object (YSO) jets (Garcia et al. 1999; Takami et al. 2001, 2002, 2003; Whelan et al. 2004; Davis et al. 2003) and the disc structure (Takami et al. 2001, 2003). The main advantage of SA is that it allows us to trace the spatial structure of an unresolved object at scales well below the seeing or diffraction limit of the telescope. This is achieved by measuring the centre of the PSF as a function of wavelength (known as a position spectrum) and measuring the displacements of emission and/or absorption feature centroids with respect to the centroid of the continuum. The presence of any displacements implies a different origin of the line emission/absorption features with respect to the continuum source. In a theoretical scenario, the accuracy of these measurements will only depend on photon statistics, i.e., the measured error will be proportional to the seeing length of the image and inversely proportional to the square root of the detected flux (Bailey 1998a). For normal sky conditions, a well exposed image can give an accuracy of a few milli-arcseconds. Detailed studies of the closest young stars using this technique have resulted in new insights into the close environments of low-mass YSOs.

In studies of star formation, massive young stars remain poorly understood. The close environment of a massive young star is much more complex than that of a low mass star due to the additional presence of ultra-compact HII (UCHII) regions and ionised winds along with disks and outflows. The relatively larger distances at which they are generally situated have made observations of these complexities very difficult. In this paper we exploit the potential of SA in unveiling the complex structure of the close environment of young massive stars. Our method involves measuring the spatial asymmetry of various emission lines representative of different physical entities such as disk, UCHII region and jets/winds using SA. For this purpose we have utilised the VLT archival near-infrared (NIR) spectra available from a NIR spectroscopic survey of massive young stellar objects (MYSOs) by Bik et al. (2006).

2. Data selection and analysis

The Bik et al. (2006) survey consists of observations with the ISAAC camera mounted on the VLT UT1 instrument, using a long slit (120″) with a width of 0.3″ resulting in a spectral resolution of $R = 8900$. We obtained these data from the ESO Science Archive Facility. Although several tens of source spectra are available from this survey, the intense nebular emission from the HII regions surrounding young massive stars and source multiplicity limit the usable sample for the purpose of SA. By excluding such effects, we found eight relatively clean single sources with low contamination from the nebular lines that were suitable for SA analysis. Of these eight sources, four sources, namely 08576-4334nr292, 18449-0158nr335, 18006-2422nr766 and 16164-5046nr3636 reveal SA signals and are discussed here. 18449-0158nr335 is a Wolf-Rayet star whereas the other three sources are MYSOs. K band spectra in the range 2.069 μm–2.189 μm were available

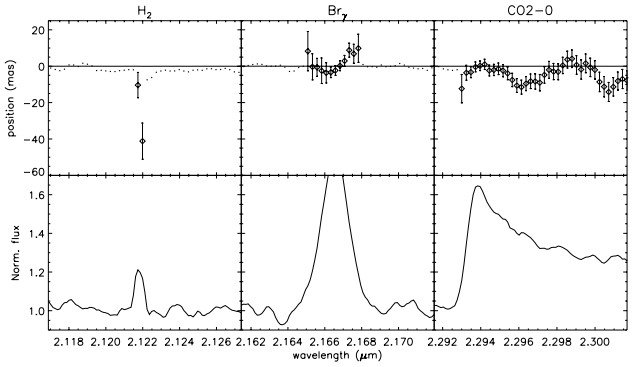

Fig. 1. Position spectra (*top*) and normalised intensity spectra (*bottom*) for the lines H_2, Brγ and CO 2–0 bandhead of the source 08576-4334nr292. In the top panel, diamonds correspond to the position spectra and dots represent the raw continuum positions. The solid line shows the fitted continuum position.

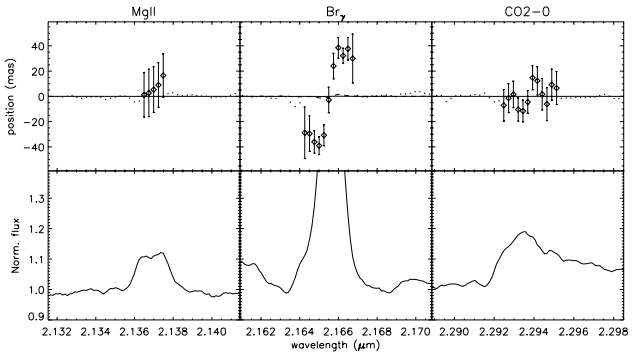

Fig. 2. Same as Fig. 1 for the source 16164-5046nr3636. The dashed line in Brγ panel shows the synthetic data computed using Eq. (6) of Brannigan et al. (2006).

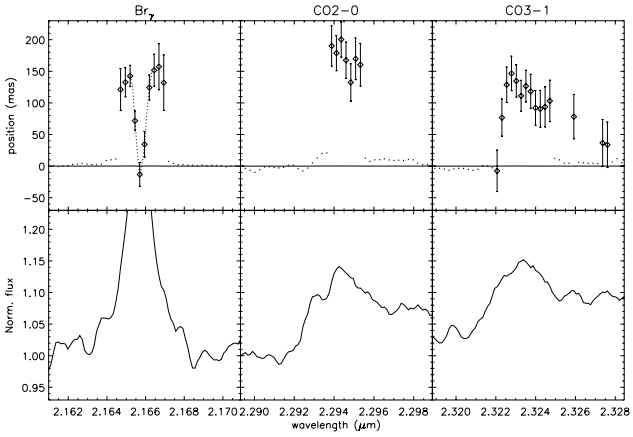

Fig. 3. Same as Fig. 1 for the source 18006-2422nr766. The dotted line in Brγ marks the region of residual nebular emission.

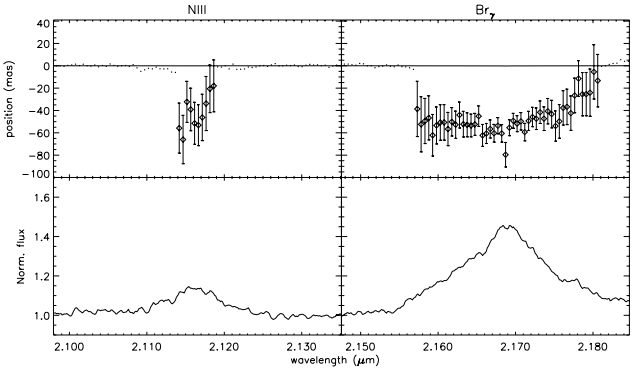

Fig. 4. Same as Fig. 1 for the source 18449-0158nr335.

for all the sources. For all but 18449-0158nr335, spectra centred at 2.234 μm covering the first CO overtone bands were also available.

The raw data obtained from the archive were reduced using standard spectroscopic reduction techniques. Fringing effects were carefully removed and the SA analysis was carried out on each exposed frame. This is necessary because errors in combining the individual exposures in a standard way can mask the SA signal. Position spectra were extracted from individual exposures of each source and combined in order to improve the S/N of the SA signal. To cancel instrumental effects in the position spectra and obtain a reliable SA signal, one has to obtain spectra at anti-parallel position angles on the same source (Bailey 1998b). This is especially relevant to remove artifacts on the position spectrum of the emission/absorption lines. However, even when spectra were limited to one or two position angles, SA analysis has been successfully carried out by fitting a polynomial function to the continuum position and subtracting it from the raw position spectrum (Davis et al. 2003; Whelan et al. 2004). This allows us to correct for curvature and tilt of the spectral image. In our trial case we adopt this method in the following way: the raw position spectrum was divided by the weighting factor of the continuum which is defined as

$$I_{\lambda(\mathrm{line})}/[I_{\lambda(\mathrm{line})} + I_{\lambda(\mathrm{cont})}] = [1 + I_{\lambda(\mathrm{cont})}/I_{\lambda(\mathrm{line})}]^{-1}, \quad (1)$$

where $I_{\lambda(\mathrm{line})}$ is the intensity of the line and $I_{\lambda(\mathrm{cont})}$ is the intensity of the continuum (Takami et al. 2001). The final position X_λ is obtained by

$$X_\lambda = (X_{\lambda(\mathrm{raw})} - X_{\lambda(\mathrm{cont})}) \cdot (1 + I_{\lambda(\mathrm{cont})}/I_{\lambda(\mathrm{line})}) \quad (2)$$

where $X_{\lambda(\mathrm{raw})}$ is the raw position and $X_{\lambda(\mathrm{cont})}$ is the fitted continuum position. The accuracy of the final position spectrum is obtained by computing the error on Eq. (2). Only those signals that were above 10% of the continuum level are treated as lines for computing the position spectra. Any signal below this level is simply treated as continuum.

3. Results

The aim of our experiment is to constrain the physical size scales from which different representative lines are produced in the circumstellar environment of a young massive star. SA directly measures the asymmetry of the emission line regions about the centroidal continuum position and not the actual size. For instance, if the geometry and kinematics of the emission line regions are spherically symmetric, no SA signal will be detected. However, it is extremely rare to find a spherically symmetric YSO. The environment surrounding a YSO is usually asymmetric, due to the clumpy nature of the molecular cores from which they form and asymmetries are more prominent around MYSOs and also are commonly observed for UCHII regions (e.g. Kurtz et al. 2004). Even in the case of low mass stars, which are relatively more symmetric, the inclination of the YSO to the line of sight, in combination with the extinction provided by the circumstellar envelope will invariably produce an asymmetry in the

Table 1. Details of the studied sources.

Name	RA(2000)	Dec(2000)	d	$FWHM$	displacement (AU)				M	i	T_{ex}
			(kpc)	($''$)	NIII	Brγ	CO 2–0	CO 3–1	($M_\odot$)	($\circ$)	(K)
08576-4334nr292	08:59:21.58	–43:45:31.5	0.7	0.60, 0.47	–	–	13 ± 4	–	6	27	1660
16164-5046nr3636	16:20:11.31	–50:53:25.3	3.6	0.92, 0.63	–	279 ± 10	134 ± 11	–	30	30	4480
18006-2422nr766	18:03:40.29	–24:22:39.6	1.9	0.83, 0.84	–	247 ± 23	311 ± 32	210 ± 39	11	60	1800
18449-0158nr335	18:47:36.66	–01:56:34.0	4.3	1.08	279 ± 21	370 ± 13	–	–	–	–	–

The M, i and T_{ex} values are estimates from Bik & Thi (2004).

projected plane of view (Whitney et al. 2003). This asymmetry can appear as a SA signal if the envelope is in emission rather than simply scattering the star light as in the case of Whitney et al. (2003). This is because the emission line centroid will be a result of envelope geometry alone whereas the continuum centroid will be due to the star+envelope contributions for the observer.

Alternatively, SA displacements can also be attributed to companion emission line stars. As we shall discuss in the next section, this is a less likely scenario for the sample of MYSOs. CO band head emission is known to arise in the disks of low mass stars (Carr 1989) and recently shown to be present in MYSOs (Bik et al. 2006). The number densities in MYSOs are generally of the order of 10^6–10^7 cm^{-3} (e.g. Mueller et al. 2002) and can peak by a few orders of magnitude locally for luminous sources with $L > 10^4\ L_\odot$, implying that the inner regions of envelopes around MYSOs have the required densities to produce CO emission. SA displacements measured from Brγ and CO band head emission lines can therefore constrain the physical dimensions of inner ionised regions and disks around MYSOs. Similarly, H_2 lines which are representative of shocked or fluorescent emission (Smith 1994) can constrain sizes of jets/outflows and/or accreting columns of the envelope.

In Figs. 1–4 the lower panel shows the intensity spectra and the upper panel shows the position spectra for the sources 08576-4334nr292, 16164-5046nr3636, 18006-2422nr766 and 18449-0158nr335 respectively. The various columns displays data for different emission lines as indicated at the top of each column. It can be seen that the SA displacements have various shapes and magnitudes for different sources and emission lines. The non-repetitive nature of the SA signal in various sources and for different emission lines, despite all the observations originating from the same instrument and telescope configuration, suggests that these SA signals are real rather than artifacts from the applied method of analysis. The error bars in each figure represent the errors of Eq. (2). It can be seen from these figures that most emission lines display SA signals. Any displacement that is larger than the measured uncertainties of the fitting is treated as a true signal.

The Brγ SA signal from the source 16164-5046nr3636 imitates the shape of an artifact described by Brannigan et al. (2006). We therefore used the intensity spectra of this source, assumed a seeing of 0.9$''$ and a PSF similar to the observed PSF and compatible with a binary with a maximum separation of 0.84$''$ and generated a synthetic SA signal using Eq. (6) of Brannigan et al. (2006). This signal shows an angular displacement of 0.003$''$ and it is overplotted on the observed Brγ signal in Fig. 2. Since the latter is much larger in magnitude than the synthetic model of artifact, we believe that this displacement is real.

SA measures the centroids of the line emitting regions that are expected to trace the mid-points and/or centre-of-gravity points, thus providing lower limits to the actual dimensions of the projected view. This is true only when the centroidal position of the continuum is located within the emission line region, as is most likely in the case of observed MYSOs. Although all the analysed data are shown in the figures, only the true signals as defined above are translated into projected physical dimensions and listed in Table 1. In the following we describe possible interpretations of the SA signal in each source.

08576-4334nr292: This source shows H_2, Brγ and CO 2–0 line emission, representative of shocked/fluorescent gas, an ionised region and a disk/envelope, but the SA signal is not prominent according to the criteria described above. The CO 2–0 line SA signal may be real since the average positional displacement is slightly above the 3σ limit. The displacement is spread on either side of the continuum reference, measuring 13 ± 4 AU when projected at the source distance of 0.7 kpc.

16164-5046nr3636: This is the most massive of the three MYSOs examined in this work. Along with Brγ emission, this source also displays MgII line representative of high temperature and possibly representing an O star candidate. Only the Brγ line shows a significant SA signal with the blue-shifted and the red-shifted parts of the line profile displaced in opposite directions with respect to the continuum source. Such a profile can be the result of an expanding shell or a bipolar outflow. Since Brγ lines are known to trace ionised material, and are not found in outflows, the most likely explanation is therefore an expanding shell around the central star due to an UCHII region or a wind.

18006-2422nr766: This source displays intense Brγ and CO bandhead emission indicative of an ionised region and a molecular disk/envelope. The source is embedded in an active massive star forming HII region, M8. The SA signals measured from Brγ, CO 2–0 and CO 3–1 are all significant and are found to be displaced towards one side of the source. The projected dimensions of these displacements are 247 ± 23, 210 ± 39 and 311 ± 32 AU for Brγ, CO 3–1 and CO 2–0 respectively. These size scales suggest a scenario where the central star is surrounded by an ionised shell, both of which are enclosed in a molecular envelope made of CO, with the CO 3–1 emitting region placed interior to the CO 2–0 emitting region. However, the displacement of all these emissions towards one side of the continuum suggests that these shells/envelopes are partially extinguished or display an asymmetrical shape about the continuum. We propose two alternate scenarios to explain this result. Asymmetric emission due to local clumping or due to the inclination effect described in the beginning of this section can explain the observed SA signal for an inclination angle in between a pole-on and edge-on configuration (see Fig. 12a in Whitney et al. 2003). In this case, although the star and the surrounding UCHII region can themselves be bright at 2 μm, a large CO envelope with an inner cavity can provide significant extinction at intermediate line-of-sight angles to imitate the effects discussed by Whitney et al. (2003). Alternatively, YSOs

immersed in intense UV fields caused by HII regions tend to produce envelopes elongated on one side such as proplyds in the Orion Nebula (see for example simulations by Richling & Yorke 2000). Interestingly, a bright OB star is situated 3.5″ away (equivalent to a projected distance of 7000 AU) to the opposite side of the line emission displacements, as observed on the slit. However, this star could be a coincidence in the line of sight and the available data is insufficient to determine any particular scenario.

18449-0158nr335: This source is a Wolf-Rayet star displaying the emission lines CIV, NIII and Brγ. No data is available to ascertain the presence/absence of any lines characteristic of molecular emission. The CIV line is not bright enough to carry out SA analysis but the NIII and Brγ lines show reasonable SA signals projecting to size scales of ∼300 and 400 AU respectively and displaced towards one side of the source. Wolf-Rayet stars are known to display asymmetrical mass loss due to fast rotation and/or companion stars. There is a faint star located 1.5″ to the south of this source (also seen on the slit) emitting CIV and Brγ but not the NIII line. These emission features common to both stars and a projected separation of 7500 AU may suggest that the faint star is a true companion to the primary Wolf-Rayet source. However, more concrete evidence is required.

4. Discussion

We have tested the applicability of the technique of spectro-astrometry to study the close environment of massive stars using a small sample of archival VLT spectra. As shown in the previous section, characteristic emission lines from ionised and molecular regions display different SA displacements, constraining the physical dimensions of the emitting regions. In a classical application of SA to study spectroscopic binaries and nearby low mass YSOs, the kind of SA displacements shown in Figs. 3 and 4 would be attributed to the presence of companion stars with line emission. In the present case, the analysis is that of a sample of MYSOs and emission lines characteristic of high temperatures that can be produced in extreme conditions involving ionization. While MYSOs are generally associated with clustering, close companions at the level of a few hundred AUs are not known. Companions due to fragmentation at similar size scales close to a MYSO that is surrounded by hot gas is also not viable according to the Jeans criteria (e.g. Kumar et al. 2003). At the typical distances of a few kpc at which these MYSOs are located, only a very luminous object such as another MYSO can produce the observed Brγ line intensities. Therefore, we do not attribute the SA displacements of the MYSOs to binary companions, although it will be an interesting experiment to pursue for future studies.

These size measurements are lower estimates to the actual dimensions since the SA technique measures the centroid of the emission rather than the edges. The listed values in Table 1 ($\sim 10^2$ AU) are similar to the estimated sizes of inner disks according to numerical simulations of MYSOs (e.g. Yorke & Sonnhalter 2002) but smaller than the sizes of toroids ($\sim 10^3$ AU) observed around MYSOs (Cesaroni et al. 1999; Beltrán et al. 2005). In comparison, the estimates from Bik & Thi (2004) are much smaller (few AU). A proper understanding of the true nature of the circumstellar environment of the MYSO can be made only by combining the different views obtained from multiple methods of investigation from the millimetre to the NIR wavelengths. The SA measurements can be very useful to provide the size scales based on NIR observations tracing the very hot and inner regions of the MYSOs and provide alternative ways to evaluate the consistency of results obtained using other methods. For example, the three MYSOs examined in this work have been analysed by Bik & Thi (2004). These authors modelled the CO line profile of the band head emission in the framework of Keplerian rotation. They arrive at disk radii of ∼3–4 AU for the sources 16164-5046nr3636 and 18006-2422nr766, for certain assumed inclination angles. In contrast, our SA analysis for the same sources indicates radii of a few hundred AU which are representative of much larger disks (not necessarily Keplerian) and/or envelopes around MYSOs. Also, the SA method yields different envelope radii traced by CO 2–0 and CO 3–1 band heads for the source 18006-2422nr766, implying the origin of these lines in regions with different physical conditions. These contrasting results between SA and line profile modelling may imply a scenario in which the massive young star is surrounded by an optically thick inner disk and an outer envelope.

The experimental application of SA demonstrates the potential of this technique in revealing details of the close environment of MYSOs. The results presented here are only indicative, based on spectra obtained at one position angle. If systematic SA observations in multiple position angles are obtained on a larger sample of MYSOs, the results can be invaluable in understanding the complex environment of MYSOs. SA is also an efficient and inexpensive method that needs only limited amounts of telescope time. In contrast, techniques such as infrared interferometry with very large telescopes and/or mm wave interferometric imaging consume large amounts of telescope time and analysis efforts to probe the same regions.

Acknowledgements. We gratefully acknowledge Paulo Garcia for a code that served to verify the existence of artifacts. We thank the referee M. Takami for useful comments that clarified several aspects of the paper. J.M.C.G. and M.S.N.K. are supported by a research grant POCTI/CFE-AST/55691/2004 and JMCG is supported by a doctoral fellowship SFRH/BD/21624/2005 approved by FCT and POCTI, with funds from the European community programme FEDER. This work is based on data obtained with ESO facilities at Paranal that was retrieved using the ESO Science Archive Facility.

References

Bailey, J. A. 1998a, Proc. SPIE, 3355, 932
Bailey, J. 1998b, MNRAS, 301, 161
Baines, D., Oudmaijer, R. D., Porter, J. M., & Pozzo, M. 2006, MNRAS, 367, 737
Beltrán, M. T., Cesaroni, R., Neri, R., et al. 2005, A&A, 435, 901
Bik, A., & Thi, W. F. 2004, A&A, 427, 13
Bik, A., Kaper, L., & Waters, L. 2006, A&A, 455, 561
Brannigan, E., Takami, M., Chrysostomou, A., & Bailey, J. 2006, MNRAS, 367, 315
Carr, J. S. 1989, ApJ, 345, 522
Cesaroni, R., Felli, M., Jenness, T., et al. 1999, A&A, 345, 949
Davis, C. J., Whelan, E., Ray, T. P., & Chrysostomou, A. 2003, A&A, 397, 693
Garcia, P. J. V., Thiébaut, E., & Bacon, R. 1999, A&A, 346, 892
Kumar, M. S. N., Fernandes, A. J. L., Hunter, T. R., Davis, C. J., & Kurtz, S. 2003, A&A, 412, 175
Kurtz, S. E., Churchwell, E., & Wood, D. O. S. 1994, ApJS, 91, 659
Mueller, K. E., Shirley, Y. L., Evans, N. J. II., & Jacobson, H. R. 2002, ApJSS, 143, 469
Richling, S., & Yorke, H. 2000, ApJ, 539, 258
Smith, M. D. 1994, MNRAS, 266, 238
Takami, M., Bailey, J., Gledhill, T. M., Chrysostomou, A., & Hough, J. H. 2001, MNRAS, 323, 177
Takami, M., Chrysostomou, A., Bailey, J., et al. 2002, ApJ, 568, 53
Takami, M., Bailey, J., & Chrysostomou, A. 2003, A&A, 397, 675
Whelan, E. T., Ray, T. P., & Davis, C. J. 2004, A&A, 417, 247
Whitney, B. A. 2005, Nature, 437, 37
Whitney, B. A., Wood, K., Bjorkman, J. E., & Cohen, M. 2003, ApJ, 578, 1079
Yorke, H. W., & Sonnhalter, C. 2002, ApJ, 569, 846